Published in final edited form as:
Mol Cell Neurosci. 2009 July ; 41(3): 304–312. doi:10.1016/j.mcn.2009.04.001.

Phr1 regulates retinogeniculate targeting independent of activity and ephrin-A signalling

Susan M. Culican, MD, PhD[1,#], **A. Joseph Bloom, PhD**[2,#], **Joshua A. Weiner, PhD**[3], and **Aaron DiAntonio, MD, PhD**[2,*]

1 *Department of Ophthalmology and Visual Sciences, Washington University School of Medicine*

2 *Department of Developmental Biology, Washington University School of Medicine*

3 *Department of Biology, University of Iowa*

Abstract

Proper functioning of the mammalian visual system requires that connections between the eyes and their central targets develop precisely. At birth, axons from the two eyes project to broad, overlapping regions of the dorsal Lateral Geniculate Nucleus (dLGN). In the adult, retinal axons segregate into distinct monocular regions at stereotyped locations within the dLGN. This process is driven by both molecular cues and activity-dependent synaptic competition. Here we demonstrate that *Phr1*, an evolutionarily conserved regulator of synapse formation and axon guidance, defines a novel molecular pathway required for proper localization of retinogeniculate projections. Following conditional excision of *Phr1* in the retina, eye-specific domains within the dLGN are severely disturbed, despite normal spontaneous retinal wave activity and monocular segregation. Although layer placement is dramatically altered, *Phr1* mutant retinal axons respond to ephrin-A *in vitro*. These findings indicate that *Phr1* is a key presynaptic regulator of retinogeniculate layer placement independent of activity, segregation, or ephrin-A signaling.

Keywords

LGN; mapping; segregation; retinal activity; mouse; presynaptic

Introduction

In binocular mammals, each dorsal lateral geniculate nucleus (dLGN) receives projecting axons from both eyes that initially form broad overlapping patches which later segregate into eye-specific layers with stereotyped shapes and locations. Both the segregation of inputs and the localization of eye-specific regions are dependent on spontaneous activity in the developing retina (Penn et al., 1998, Muir-Robinson et al., 2002). In ferrets, pharmacologic elimination of all retinal activity results in minor alteration of the location of retinal inputs, with most of the inputs occupying the stereotypically appropriate region of the dLGN, suggesting a role for

*Corresponding author: Aaron DiAntonio.
#These authors contributed equally.
Correspondant Footnote: Aaron DiAntonio, Department of Developmental Biology, Box 8103, Washington University School of Medicine, 660 S. Euclid Ave, St. Louis, MO 63110, Phone: (314)-362-9925, Fax: (314)-362-7058, Email: diantonio@wustl.edu

activity independent mechanisms that modulate the localization of inputs (Cook et al., 1999). Indeed, in triple knockout mice that lack all ephrin-A ligands, spontaneous retinal activity and monocular segregation are preserved, but the location and shape of eye-specific patches are dramatically altered (Pfeiffenberger et al., 2005).

Phr1 and its orthologs are huge, multi-domain proteins that play a central role in neural development. Loss of PHR proteins lead to excess synaptic growth in Drosophila (Wan et al., 2000; DiAntonio et al., 2001), synaptogenesis and axon termination defects in C. elegans (Schaefer et al., 2000; Zhen et al., 2000), and axon guidance defects in in both invertebrates and vertebrates (Burgess et al., 2004; Bloom et al., 2007; Lewcock et al., 2007; Hendricks et al., 2008). In zebrafish, mutation of the *Phr1* ortholog *esrom* leads to multiple defects in retinal projections including abnormal axonal bundling, midline crossing, target selection, mapping, and segregation (D'Souza et al., 2005). In mouse, constitutive *Phr1* mutants die perinatally and display abnormal neuromuscular junction morphology and severe guidance defects of motor, cortical, and thalamic projections through a combination of cell autonomous and non-autonomous mechanisms (Lewcock et al., 2007; Bloom et al., 2007). Hence, PHR proteins control the development of major axon tracts in the brain, as well as the fine structure of individual synapses.

To determine whether *Phr1* regulates postnatal mechanisms that refine neuronal connectivity, we have used the Cre-lox system to conditionally inactivate *Phr1* in the retina while preserving *Phr1* function in the rest of the CNS. In the absence of *Phr1* in the retina, retinal development appears undisturbed; mutant retinas retain their normal lamination and generate spontaneous waves of activity. Mutant retinal ganglion cell (RGC) axons respond appropriately to the optic chiasm, target the dLGN, and segregate into eye-specific domains. Stereotyped layer placement, however, is severely disrupted. Indeed, loss of *Phr1* in the eye leads to dramatic errors in the location of retinal projections within the dLGN that are very similar to those present in triple ephrin-A knockout mice (Pfeiffenberger, 2005). Despite this similarity in phenotypes, *Phr1* mutant retinal axons still respond to ephrin-A *in vitro*. These findings indicate that *Phr1* is an important presynaptic regulator of axonal targeting independent of activity, segregation, or ephrin-A signaling.

Results

Gross Retinal Development is Preserved in *Phr1* retinal mutants

Phr1 mRNA is highly expressed in the retina (Figure 1A–C). Constitutive *Phr1* knockout mice die at birth before much of retinal development occurs, so to examine retinal phenotypes we crossed the *Phr1* conditional mutant (Bloom et al., 2007; Figure 1D) with *Math5-Cre* mice (Yang et al., 2003). In these mice Cre is expressed in RGCs as well as amacrine and horizontal cells, generating *Phr1* retinal mutants. The organization of the resulting *Phr1* mutant retinas appeared grossly normal. There were no quantitative or qualitative differences in the size, structure, or thickness of cellular and plexiform layers, and the expression of appropriate molecular markers for cell bodies and synapses (Figure 1E–H). Thus, loss of *Phr1* does not cause gross defects within the retina.

Localization of the ipsilateral retinogeniculate projection is abnormal in *Phr1* retinal mutants

We previously observed a failure of retinal innervation of the thalamus in constitutive *Phr1* stillborn pups using DiI tracing (Bloom et al., 2007). Subsequent analysis in late embryos, however, demonstrated that RGC axons can project to the thalamus (data not shown) suggesting that previous findings were likely complicated by axonal degradation in the dying pups. To clarify the role of *Phr1* in postnatal retinogeniculate development we labeled retinogeniculate axons from conditional *Phr1* retinal mutants with fluorescently tagged cholera toxin (CTB).

RGC projections to the suprachiasmatic nucleus, dLGN and superior colliculus are grossly normal in *Phr1* retinal mutants, with neither ectopic nor missing projections. Because the dLGN receives input from both eyes, ipsi- and contra-laterally projecting RGC axons were visualized independently by injecting each eye with different CTB conjugates. In wild-type adult mice the ipsilateral projection occupies a stereotypical region in the dorsomedial quadrant of the dLGN, with the remainder of the nucleus innervated by the contralateral eye (Figure 2A). In retinal *Phr1* mutants RGC projections also fill the dLGN and segregate into eye-specific domains, but the ipsilateral projection is dramatically altered in shape and location (Figure 2B,C). The ipsilateral projection in the *Phr1* retinal mutant is variable in its location and shape, often demonstrating multiple patches instead of the typical single patch seen in control animals (Figure 2, arrows). When a single patch is observed it is commonly infero-laterally displaced and orthogonal to the orientation of the nucleus. Localization to the inferior portion of the nucleus is also observed (Figure 3, arrows). While the phenotype is not stereotypical in that the position of the ipsilateral patch varies, it is robust. In classifying the genotype based upon the projection phenotype, two observers (H and S) were correct 100% of the time. A third observer (J) was correct 92% of the time (95% CI = 81%–100%; n=72 observations).

Math5-Cre is pan-retinal but it is also expressed in regions of the brain, although *Math5-Cre* expression has not been reported in the thalamus (Hufnagel, 2007). To test the hypothesis that loss of *Phr1* from the retina alone results in our phenotype, we compared *Math5*-Cre retinal *Phr1* mutants to those made using another retina-expressing Cre line, *alphaPax6-Cre* (Pax-Cre; Marquardt et al., 2001). Pax-Cre expression is restricted to the retina alone. Within the retina Pax-Cre is expressed in a mosaic pattern across the retina, with reduced density of Cre expressing cell-bodies in a narrow dorso-medial wedge, but strong expression in the ventral-temporal RGCs that project to the ipsilateral dLGN (Stacy et al., 2005). We confirmed Cre expression patterns using a *Thy1-Stop-YFP* Cre-inducible marker (YFP-15, Buffelli et al., 2003; Figure 3). YFP-labeled retinal projections densely innervated the dLGN in both Cre lines (data not shown). To test the hypothesis that it is the loss of *Phr1* from the retina alone that leads to the mislocalization of the ipsilateral patch, we compared retinal mutants made using RGC ubiquitous *Math5*-Cre and retina-specific Pax-Cre. Mapping defects in *Phr1* retinal mutants using *Math5*-Cre were indistinguishable from those obtained with Pax-Cre (Figure 2). Hence, *Phr1* excision in retina alone is sufficient for the phenotype, demonstrating that the eye-specific domain placement error is due to a cell-autonomous requirement for *Phr1* in RGCs.

Mislocalization of ipsilaterally projecting RGCs cannot be explained by aberrant crossing at the optic chiasm

The mislocalization of the ipsilateral patch in *Phr1* retinal mutants may be the result of abnormalities in the number of axons projecting to the ipsilateral LGN resulting in a change in the ratio of inputs between the two eyes. To test this possibility we measured the area occupied by the ipsilateral projection in controls and both retinal mutants and found that it is unaffected (14.61% +/− 1.43% no Cre; 12.46% +/− 1.24% Pax-Cre; 14.64% +/− 1.09% *Math5*-Cre; Figure 2D; Figure 4), indicating that the mislocalization is not associated with an altered balance of inputs between the eyes. Another potential explanation for the misplacement of eye-specific layers in the dLGN is altered routing through the optic chiasm: aberrantly crossing axons could innervate their *correct* positions in the *wrong* dLGN. To investigate this possibility we retrogradely labeled retinas by injecting CTB into the dLGN. Both in controls and *Phr1* retinal mutants, axons projecting to the ipsilateral dLGN originate primarily from the inferotemporal retina (Figure 5) Hence, inferotemporal RGCs project to the ipsilateral dLGN as usual, so mapping defects in *Phr1* retinal mutants are not secondary to guidance errors at the optic chiasm.

Spontaneous wave activity and monocular segregation are preserved in *Phr1* retinal mutants

Projections from both eyes to the dLGN are initially highly intermingled then segregate into eye-specific regions via an activity-dependent process over the first few postnatal weeks in mice. Mutations that cause abnormal retinal activity or delayed monocular segregation can lead to aberrantly organized monocular domains (Muir-Robinson et al., 2002). To determine whether abnormal retinal activity could account for the abnormal placement of the ipsilateral projection, we analyzed retinal activity in the absence of *Phr1*. Both mutant and control retinas show spontaneous correlated wave activity at P10 (Figure 6C). Although the frequency of bursting activity is variable in both controls (mean 0.422+/−0.024; range 0.333–0.533 waves/min) and mutants (mean 0.456+/− 0.062; range 0.333–0.533 wav/min), no consistent difference between genotypes is observed (t-test, p=0.543). Furthermore, normal spatial visual acuity in *Phr1* retinal mutants, tested using a virtual optomotor system, is indirect evidence that normal retinal activity is preserved in adults. Both controls and mutants respond to approximately 0.4 cyc/degree (data not shown), consistent with published reports for normal adult vision (Prusky et al., 2004).

Because eye-specific segregation is driven by spontaneous activity in the retina (Penn et al., 1998), and retinal activity is normal in the *Phr1* retinal mutants, we expected that segregation of inputs was also normal. To assess segregation of inputs directly, we examined animals from P4 to adult (Figure 6A). Quantitative image analysis (Torborg and Feller, 2004) demonstrates that progression of segregation of ipsi- and contralateral inputs in *Phr1* mutants is indistinguishable from littermate controls (Figure 6B). Despite this normal time course, localization of the ipsilateral input during segregation is disturbed. Taken together, these results demonstrate that *Phr1* is not required for normal retinal wave activity or timely eye-specific segregation.

Phr1 mutant RGC axons exhibit aberrant morphology but respond appropriately to ephrin-A *in vitro*

Triple ephrin-A knockouts display an aberrant placement of eye-specific projections that is very similar to the *Phr1* phenotype (Pfeiffenberger et al., 2005). Therefore, we assessed whether loss of *Phr1* alters the normal gradient of EphA receptors across the retina, i.e. highest EphA expression temporally to lowest EphA expression nasally (Feldheim et al, 1998). Affinity probe *in situ* with an ephrin-A5 ligand fusion protein demonstrates that the gradient persists in the *Phr1* mutant at P0 (Figure 7A). Thus, the *Phr1* mapping defect is not due to the abolishment of a retinal EphA receptor gradient and demonstrates that mutant retinas retain the positional information necessary to generate molecular gradients.

To test whether axons lacking *Phr1* can respond to ephrin-As, explants from *Phr1* constitutive mutant and littermate control retinas were cultured in an ephrin-A border assay (Petros et al., 2006). Cultured mutant axons display morphological defects reminiscent of *Phr1* phenotypes observed at neuromuscular junctions (Burgess et al., 2004, Bloom et al., 2007) and in cultured motoneuron axons (Lewcock et al., 2007) including bulbous protrusions along axon shafts and at growth cones, and abnormally kinked axonal trajectories (Figure 7B,C). However, no difference in ephrin-A responsiveness is observed: both control and mutant explants grown directly upon ephrin-A-conjugated substrate extend far fewer axons than without ephrin-A (data not shown), and axons grown on ephrin-free substrate show a marked reluctance to cross into ephrin-A-conjugated territory (Figure 7D,E) leading to an approximately five-fold reduction in axon density within the ephrin-A-containing regions for both control and mutant explants (*Phr1* KO=21±5%, n=5 explants; Control=21±3%, n=14; Figure 7G,H). In contrast, axons were not repulsed by a BSA-only conjugated border, growing equally well on the culture substrate and on BSA (Figure 7F). Therefore, despite the similarity between the ephrin-A triple knockout and *Phr1* retinal knockout retinogeniculate mapping defects *in vivo*, the *Phr1*

phenotype can not be explained simply as a functional ephrin-A signaling knockout in RGC axons. While subtle defects in ephrin-A responsiveness cannot be excluded, these results are consistent with the contribution of *Phr1* to an ephrin-A-independent mechanism for axon localization in the retinogeniculate system.

Discussion

Phr1 and its orthologs are huge, multi-domain proteins with well-characterized roles in synapse development and axon guidance. Here we use conditional excision in the retina to demonstrate the requirement for *Phr1* in the proper formation of the retinogeniculate projection in mouse.

In binocular mammals ipsilateral and contralateral retinal projections initially innervate the dLGN in broad, overlapping patches that reorganize postnatally to become eye-specific layers with stereotyped shapes and locations. Here we demonstrate that retinal expression of *Phr1* is required for proper localization of retinogeniculate projections but not for eye-specific segregation. When *Phr1* is deleted in the retina, mutant RGCs project to an improper region of a genetically intact dLGN. The *Phr1* mutant retina retains its normal lamination pattern and shows normal expression of a variety of synaptic and dendritic markers. Mutant RGC axons respond appropriately to the optic chiasm, with axons from the inferotemporal retina projecting to the ipsilateral thalamus as in wild type. The mutant retina generates spontaneous waves of activity, and the projections segregate into eye-specific domains on a normal time course.

Correct layer placement in the dLGN requires acetylcholine receptors (Muir-Robinson et al., 2002), nyctalopin (Demas et al., 2003), L-type Ca channels (Cork et al., 2001), Ten-m3 (Leamey et al., 2007), BMPs (Plas et al., 2008), and ephrin-As (Pfeiffenberger et al., 2005). Among these mutants, the mislocalization phenotype of the triple ephrin-A knockout is most similar to the *Phr1* knockout phenotype, with a well-segregated ipsilateral patch identical in size to the wild-type patch but severely altered in shape and location along the dorsal-lateral to ventral-medial axis. In addition, only ephrin-A and *Phr1* have been demonstrated to exert their effects independent of activity. As such, we tested the hypothesis that ephrin-A responsiveness is disrupted in the *Phr1* mutant, but found no evidence that ephrin-A signaling is disrupted in *Phr1* retinal mutants. EphA receptors are still expressed in a temporal to nasal gradient across the retina and RGC axons from the temporal retina still respond to ephrin-A in an *in vitro* border assay. This is consistent with the finding that *Phr1* mutant motor axons respond appropriately to ephrin *in vitro* (Lewcock et al., 2007). In addition, guidance of mutant retinal axons at the optic chiasm is normal, demonstrating that retinal axons *in vivo* can respond appropriately to the ephrin-B ligands at the midline (Williams et al., 2003). While we have no evidence for a change in ephrin-A responsiveness, this does not rule out a subtle, quantitative change in ephrin signaling. We note, however, that deletion of two of the three relevant ephrin-A ligands, which would likely cause such a quantitative change in EphA signaling, does not lead to mapping defect as severe as the *Phr1* mutant (Pfeiffenberger et al., 2005). Taken collectively, our data are most consistent with *Phr1* acting in an ephrin-A and activity-independent mapping pathway.

How does the *Phr1* mapping defect relate to the other molecular and cellular functions ascribed to *Phr1* and its orthologs? PHR proteins act as E3 ubiquitin ligases (D'Souza et al., 2005; Liao et al., 2004, Wu et al., 2005), but they are large proteins with many domains that possess additional functions (Pierre et al., 2004; Le Guyader et. al., 2005). Numerous genetic and biochemical targets of PHR proteins have been identified, including the mixed lineage kinase DLK/wallenda, TSC1, adenylate cyclase, and the Rab GEF GLO-4 (Nakata et al.,2005; Collins et al.,2006; Murthy et al., 2004; Guo et al., 1998, Grill et al., 2007). Of these, adenylate cyclase is a candidate effector of *Phr1* function in the retina. Adenylate cyclase activity is required for retinotopic mapping, though this is postulated to be due to the role of cAMP in generating the

retinal waves that drive segregation (Stellwagen et al., 1999). Since retinal activity and segregation are normal in the *Phr1* retinal mutant, alterations in adenylate cyclase activity are unlikely to explain the mapping defect. At the cellular level, *Phr1* regulates the axonal cytoskeleton (Lewcock et al., 2007), and mutant motoneuron and retinal axons grown in culture display an abnormal kinked morphology (Lewcock et al., 2007 and this study). While such cytoskeletal defects could affect axonal behavior, many axon guidance decisions are not disrupted: RGC axons exit the eye appropriately, form the optic nerve, make proper crossing decisions at the optic chiasm, select the appropriate thalamic nuclei, and prune their axonal arbors during activity-dependent segregation. As such, no single known role for *Phr1* explains its function in retinal ganglion cells. Instead, *Phr1* may integrate multiple signaling pathways and coordinate cytoskeletal dynamics to allow retinal ganglion cells to interpret and respond appropriately to localization cues in the dLGN by affecting targeting and branching within the terminal fields.

Experimental Methods

Mice

The *Phr1* floxed allele mice were described previously (C57BL/6; Bloom et al., 2007). Alpha Pax6-Cre mice (C57BL/6; Marquardt et al., 2001), and Thy-Stop-YFP15 mice (C57BL/6; Buffelli et al., 2003) were obtained from Joshua R. Sanes (Harvard University). Math5-Cre mice (mixed strain C57BL/6J, 129/SvEv; Yang et al., 2003) were obtained from Russell Van Gelder (University of Washington).

Immunohistochemistry, *In situ* RNA hybridization, and Affinity Probe *in situ*

Whole eye sections were prepared for histology as previously described (Weiner et al., 2004). Primary antibodies included: mouse anti-bassoon (Stressgen; 1:200); goat anti-choline acetyltransferase (ChAT; Chemicon, 1:100); rat anti-ALCAM (1:3; Weiner et al., 2004); rabbit anti-gamma aminobutyric acid (GABA; Sigma; 1:500); guinea pig anti-vesicular glutamate transporter-1 (VGlut1) and anti-VGlut2 (mixed 1:1 and used at 1:500; Chemicon); and mouse anti-Brn3a (Chemicon; 1:25). The species- and/or isotype-specific secondary antibodies coupled to Alexa 488 or 568 (Invitrogen) were used at 1:500. Antisense and sense dioxigenin labeled RNA probes were made from I.M.A.G.E. cDNA clone 1361780 (ResGen, Invitrogen Corp), a 700 bp cDNA fragment corresponding to nucleotides 10,502 to 11,169 of *Phr1* cloned into pT7T3 vector. *In situ* hybridization using the tyramide signal amplification (TSA) Plus kit (Perkin Elmer Life Sciences) was performed as previously described (Yamagata et al., 2006). Sections of whole head for affinity probe in situ were prepared and hybridized with recombinant human Ephrin-A5/Fc chimera (4 μg/ml, R&D Systems) followed by Cy3 α human (Jackson Laboratories) according to Yamagata et al. (2006).

Eye injection and visualization of the dLGN

10 μl syringes (Hamilton) were used to inject 1–2 μl of cholera toxin B (CTB) conjugated to Alexa-647 or Alexa-555 (1 mg/ml in PBS; Molecular Probes). Mice were sacrificed 1–2 d later and intercardially perfused with 4% paraformaldehyde in PBS, and brains fixed overnight. If the superior collilus contralateral to the injected eye was not completely outlined with fluorescence labeling the brains were considered to have incomplete fills and were not used for quantitative analysis. 80–100 μm coronal sections were cut using a vibratome.

Thalamus injection and visualization of the retina

Anesthestized mice were restrained in a steriotactic aparatus. The scalp was treated with Betadine, opened along the midline, and the skull trephined 2.5 mm posterior of Bregma and 2 mm from the midline. Approximately 0.1 μl of conjugated choleratoxin was injected into the

brain using a Picospritzer III injection system (Parker Hannifin). Animals were sacrificed and brains were prepared as for eye injections. Retinas were dissected out flat, and whole-mounted in 70% glycerol.

Quantification of size and overlap of projections

Measurements and quantification were performed according to Torborg and Feller (2004). Breifly, to determine the size of the dLGN and the spatial extent of the projections, images were background subtracted, thresholded and binarized (Image J) and the boundaries of the dLGN defined. Binary images were used only to determine the sizes of the patches. Analysis of segregation of ipsilateral and contralateral axons was done using the threshold-independent approach of generating R-distributions for each pixel and evaluating the variance of those R values at each age. For each pixel in the image an R-value was calculated by taking the $\log_{10}$ of the fluorescence intensity of the ipsilateral channel divided by the fluorescence intensity of the contralateral channel ($R= \log_{10}(F_I/F_C)$) using Matlab Software (MathWorks). The variance of all of the R-distributions for each image was calculated. Highly segregated images had a large variance in the R-distributions while less segregated images were reflected with much lower variances. Values for individual animals were calculated using the average variance of 3 to 5 successive sections through the dLGN (Figure 4). Two or three animals were analyzed for each genotype at each timepoint. Image analysis was performed blind to genotype.

Multielectrode extracellular recording from retina and acuity testing

Multielectrode array recordings were performed according to Demas et al. (2003). Briefly, retinal mutants (*Phr1* floxed-allele × Math5-Cre; n=3) and control animals (*Phr1* floxed-allele, no Cre; n=9) were sacrificed on P10 and retinas dissected and placed ganglion cell-side down in a recording chamber of 60 planar electrodes with 200 μm spacing. Custom software (Holy et al., 2000) was used to acquire and analyze the data. T-test comparisons were made after post-hoc Levene's test demonstrated equal variances in the two samples.

Spatial visual acuity was performed using a virtual optomotor system (OptoMotry; CerebralMechanics, Lethbride, Alberta, Canada) described in Prusky et al. (2004). Retinal mutants (*Phr1* floxed-allele × Math5-Cre; n=2) and control animals (*Phr1* floxed-allele, no Cre littermates; n=3) were tested with both clockwise and counter-clockwise variable spatial frequency sine wave patterns. Visual thresholds for each animal were defined as the highest spatial frequency the animal could track as determined by an observer masked to genotype.

RGC explant assays and analysis

We modified an ephrin border assay (Petros et al., 2006) using 8.5 μg/ml recombinant ephrinA2-Fc (R&D Systems), clustered with 10-fold excess of goat anti-human Fc antibody (MP Biomedicals), visualizing the border with BSA conjugated to Alexa Fluor 488 (1:100 or 1:1,000 Molecular Probes). Retinal explants were taken from the temporal third of E16 retinas, plated in Neurobasal (Invitrogen) containing BDNF (Peprotech) and B27 (Invitrogen). Cultures were grown 4–14 days, fixed 1 hour in 4% paraformaldehyde-PBS, and stained with mouse anti-pan-neurofilament cocktail (SMI 1:1,000) and Cy3 goat anti-rabbit (Molecular Probes). Only explants appropriately distant from the ephrin-A border and from other explants were chosen for quantification. The total area covered by neurites in ephrin regions adjacent to explants and equivalent non-ephrin regions were measured with Metamorph software (Universal Imaging).

Acknowledgments

We are very grateful to Rachel Wong, Josh Sanes, Paul Bridgeman, Andreas Burkhalter and Brad Miller for experimental advice and assistance. We also recognize Joseph Mertz, Sylvia Johnson, Doug Cox and Alex Barsam

for technical support. Mouse colony maintenance was managed with care by the technicians of the Washington University Animal Facility. This research was supported by the Horncrest Foundation, McDonnell Center for Higher Brain Function, and Knights Templar Foundation Awards to S.M.C. and by the Keck Foundation and NIH (DA020812) to A.D.

References

1. Bloom AJ, Miller BR, Sanes JR, DiAntonio A. The requirement for Phr1 in CNS axon tract formation reveals the corticostriatal boundary as a choice point for cortical axons. Genes Dev 2007;21:2593–606. [PubMed: 17901218]
2. Buffelli M, Burgess RW, Feng G, Lobe CG, Lichtman JW, Sanes JR. Genetic evidence that relative synaptic efficacy biases the outcome of synaptic competition. Nature 2003;424:430–4. [PubMed: 12879071]
3. Burgess RW, Peterson KA, Johnson MJ, Roix JJ, Welsh IC, O'Brien TP. Evidence for a conserved function in synapse formation reveals Phr1 as a candidate gene for respiratory failure in newborn mice. Mol Cell Biol 2004 2004;24:1096–105.
4. Collins CA, Wairkar YP, Johnson SL, DiAntonio A. Highwire restrains synaptic growth by attenuating a MAP kinase signal. Neuron 2006;51:57–69. [PubMed: 16815332]
5. Cook PM, Prusky G, Ramoa AS. The role of spontaneous retinal activity before eye opening in the maturation of for and function in the retinogeniculate pathway of the ferret. Vis Neurosci 1999;16:491–501. [PubMed: 10349970]
6. Cork RJ, Namkung Y, Shin HS, Mize RR. Development of the visual pathway is disrupted in mice with a targeted disruption of the calcium channel beta(3)-subunit gene. J Comp Neurol 2001;440:177–91. [PubMed: 11745616]
7. Demas J, Eglen SJ, Wong RO. Developmental loss of synchronous spontaneous activity in the mouse retina is independent of visual experience. J Neurosci 2003;23:2851–60. [PubMed: 12684472]
8. DiAntonio A, Haghighi AP, Portman SL, Lee JD, Amaranto AM, Goodman CS. Ubiquitination-dependent mechanisms regulate synaptic growth and function. Nature 2001;412:449–52. [PubMed: 11473321]
9. D'Souza J, Hendricks M, Le Guyader S, Subburaju S, Grunewald B, Scholich K, Jesuthasan S. Formation of the retinotectal projection requires Esrom, an ortholog of PAM (protein associated with Myc). Development 2005;132:247–56. [PubMed: 15590740]
10. Feldheim DA, Vanderhaeghen P, Hansen MJ, Frisén J, Lu Q, Barbacid M, Flanagan JG. Topographic guidance labels in a sensory projection to the forebrain. Neuron 1998;21:1303–13. [PubMed: 9883724]
11. Grill B, Bienvenut WV, Brown HM, Ackley BD, Quadroni M, Jin Y. C. elegans RPM-1 regulates axon termination and synaptogenesis through the Rab GEF GLO-4 and the Rab GTPase GLO-1. Neuron 2007;55:587–601. [PubMed: 17698012]
12. Guo Q, Xie J, Dang CV, Liu ET, Bishop JM. Identification of a large Myc-binding protein that contains RCC1-like repeats. Proc Natl Acad Sci USA 1998;95:9172–9177. [PubMed: 9689053]
13. Hendricks M, Mathuru AS, Wang H, Silander O, Kee MZ, Jesuthasan S. Disruption of Esrom and Ryk identifies the roof plate boundary as an intermediate target for commissure formation. Mol Cell Neurosci 2008;37:271–83. [PubMed: 18060805]
14. Holy TE, Dulac C, Meister M. Responses of vomeronasal neurons to natural stimuli. Science 2000;289:1569–72. [PubMed: 10968796]
15. Hufnagel RB, Riesenberg RA, Saul SM, Brown NL. Conserved regulation of Math5 and Math1 revealed by Math5-GFP transgenes. Mol Cell Neurosci 2007;36:435–48. [PubMed: 17900924]
16. Leamey CA, Merlin S, Lattouf P, Sawatari A, Zhou X, Demel N, Glendining KA, Oohashi T, Sur M, Fassler R. Ten_m3 regulates eye-specific patterning in the mammalian visual pathway and is required for binocular vision. PLOS Biol 2007;5:2077–2092.
17. Le Guyader S, Maier J, Jesuthasan S. Esrom, an ortholog of PAM (protein associated with c-myc), regulates pteridine synthesis in the zebrafish. Dev Biol 2005;277:378–86. [PubMed: 15617681]
18. Lewcock JW, Genoud N, Lettieri K, Pfaff SL. The ubiquitin ligase Phr1 regulates axon outgrowth through modulation of microtubule dynamics. Neuron 2007;56:604–20. [PubMed: 18031680]

19. Liao EH, Hung W, Abrams B, Zhen M. An SCF-like ubiquitin ligase complex that controls presynaptic differentiation. Nature 2004;430:345–50. [PubMed: 15208641]
20. Marquardt T, Ashery-Padan R, Andrejewski N, Scardigli R, Guillemot F, Gruss P. Pax6 is required for the multipotent state of retinal progenitor cells. Cell 2001;105:43–55. [PubMed: 11301001]
21. Muir-Robinson G, Hwang BJ, Feller MB. Retinogeniculate axons undergo eye-specific segregation in the absence of eye-specific layers. J Neurosci 2002;22:5259–64. [PubMed: 12097474]
22. Murthy V, Han S, Beauchamp RL, Smith N, Haddad LA, Ito N, Ramesh V. Pam and its ortholog highwire interact with and may negatively regulate the TSC1.TSC2 complex. J Biol Chem 2004;279:1351–8. [PubMed: 14559897]
23. Nakata K, Abrams B, Grill B, Goncharov A, Huang X, Chisholm AD, Jin Y. Regulation of a DLK-1 and p38 MAP kinase pathway by the ubiquitin ligase RPM-1 is required for presynaptic development. Cell 2005;120:407–20. [PubMed: 15707898]
24. Penn AA, Riquelme PA, Feller MB, Shatz CJ. Competition in retinogeniculate patterning driven by spontaneous activity. Science 1998;279:2108–12. [PubMed: 9516112]
25. Petros TJ, Williams SE, Mason CA. Temporal regulation of EphA4 in astroglia during murine retinal and optic nerve development. Mol Cell Neurosci 2006;32:49–66. [PubMed: 16574431]
26. Pierre SC, Hausler J, Birod K, Geisslinger G, Scholich K. PAM mediates sustained inhibition of cAMP signaling by sphingosine-1-phosphate. EMBO J 2004;23:3031–40. [PubMed: 15257286]
27. Pfeiffenberger C, Cutforth T, Woods G, Yamada J, Renteria RC, Copenhagen DR, Flanagan JG, Feldheim DA. Ephrin-As and neural activity are required for eye-specific patterning during retinogeniculate mapping. Nat Neurosci 2005;8:1022–7. [PubMed: 16025107]
28. Plas DT, Dhande OS, Lopez JE, Murali D, Thaller C, Henkemeyer M, Furuta Y, Overbeek P, Crair MC. Bone Morphogenic Proteins, Eye Patterning, and Retinocollicular Map Formation in the Mouse. J Neurosci 2008;28: 7057–7067. [PubMed: 18614674]
29. Prusky GT, Nazia MA, Beekman S, Douglas RM. Rapid quantification of adult and developing mouse spatial vision using a virtual optomotor system. IOVS 2004;45:4611–4616.
30. Schaefer AM, Hadwiger GD, Nonet ML. rpm-1, a conserved neuronal gene that regulates targeting and synaptogenesis in C. elegans. Neuron 2000;26:345–56. [PubMed: 10839354]
31. Stacy RC, Demas J, Burgess RW, Sanes JR, Wong RO. Disruption and recovery of patterned retinal activity in the absence of acetylcholine. J Neurosci 2005;25:9347–57. [PubMed: 16221843]
32. Stellwagen D, Shatz CJ. An instructive role for retinal waves in the development of retinogeniculate connectivity. Neuron 2002;33:357–67. [PubMed: 11832224]
33. Torborg CL, Feller MB. Unbiased analysis of bulk axonal segregation patterns. J Neurosci Methods 2004;135:17–26. [PubMed: 15020085]
34. Wan HI, DiAntonio A, Fetter RD, Bergstrom K, Strauss R, Goodman CS. Highwire regulates synaptic growth in Drosophila. Neuron 2000;26:313–29. [PubMed: 10839352]
35. Weiner JA, Koo SJ, Nicolas S, Fraboulet S, Pfaff SL, Pourquié O, Sanes JR. Axon fasciculation defects and retinal dysplasias in mice lacking the immunoglobulin superfamily adhesion molecule BEN/ALCAM/SC1. Mol Cell Neurosci 2004;27:59–69. [PubMed: 15345243]
36. Williams SE, Mann F, Erskine L, Sakurai T, Wei S, Rossi DJ, Gale NW, Holt CE, Mason CA, Henkemeyer M. Ephrin-B2 and EphB1 mediate retinal axon divergence at the optic chiasm. Neuron 2003;39:919–35. [PubMed: 12971893]
37. Wu C, Wairkar YP, Collins CA, DiAntonio A. Highwire function at the Drosophila neuromuscular junction: spatial, structural, and temporal requirements. J Neurosci 2005;25:9557–66. [PubMed: 16237161]
38. Yamagata M, Weiner JA, Dulac C, Roth KA, Sanes JR. Labeled lines in the retinotectal system: markers for retinorecipient sublaminae and the retinal ganglion cell subsets that innervate them. Mol Cell Neurosci 2006;33:296–310. [PubMed: 16978878]
39. Yang Z, Ding K, Pan L, Deng M, Gan L. Math5 determines the competence state of retinal ganglion cell progenitors. Dev Biol 2003;264:240–54. [PubMed: 14623245]
40. Zhen M, Huang X, Bamber B, Jin Y. Regulation of presynaptic terminal organization by C. elegans RPM-1, a putative guanine nucleotide exchanger with a RING-H2 finger domain. Neuron 2000;26:331–4. [PubMed: 10839353]

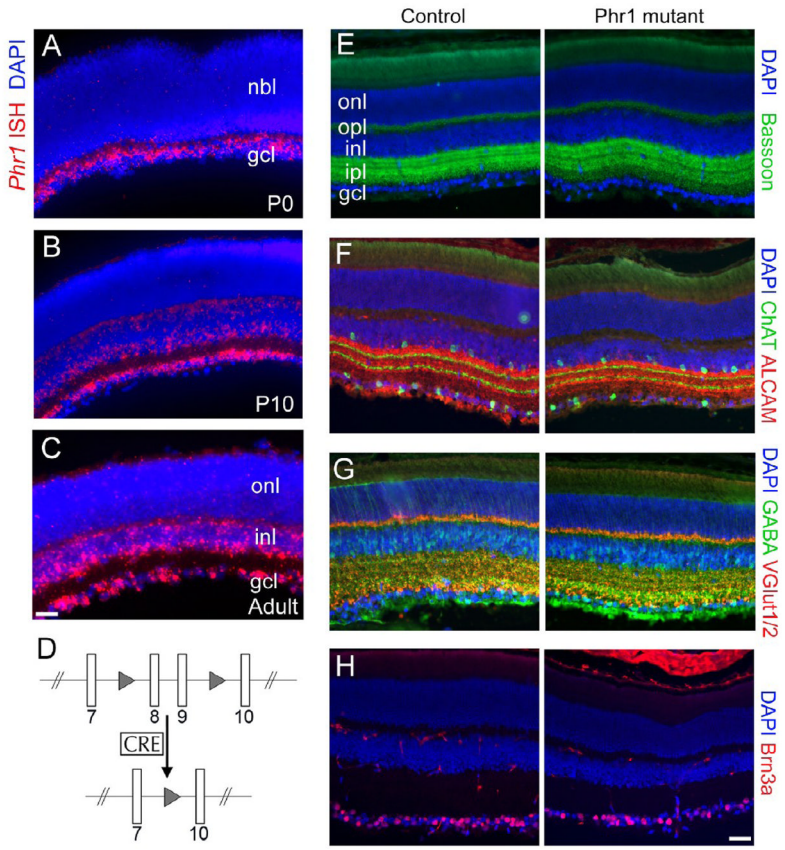

Figure 1.

Normal retinal structure in *Phr1* retinal-specific knockouts. (**A–C**) *In situ* hybridization to cross sections of wild type retinas demonstrate *Phr1* expression (red) in the retinal ganglion cell layer (gcl) at P0, P10, and in adults. As the neuroblast layer (nbl) differentiates, expression is also observed in the horizontal and amacrine cells of the inner nuclear layer (inl) at P10 and in adults. All nuclei are labeled with DAPI (blue). (**D**) Schematic of the floxed *Phr1* allele: two LoxP sites (triangles) flank the eighth and ninth exons to create the 'floxed' allele. In the presence of retina-specific Cre the two LoxP sites recombine and excise the intervening exons resulting in a knockout allele. (**E–H**) Immunohistochemistry on cross sections of retinas from P28 control (Cre-negative) and Math5-Cre-positive retinal *Phr1* knockout mice. (**E**) The presynaptic active zone marker Bassoon (green) labels the two synaptic zones of the retina, the inner plexiform layer (ipl) and the outer plexiform layer (opl). (**F**) Antibodies against the immunoglobulin superfamily member ALCAM (red) label processes in sublaminae 1, 3, and 5 of the ipl as well as some RGC axons, while ChAT (green) is a marker of cholinergic amacrine cells with terminals in sublaminae 2 and 4. (**G**) VGlut-1 and -2 (red) mark excitatory presynaptic terminals in the ipl and opl, while GABA marks inhibitory presynaptic terminals. (**H**) Brn3a (red) is a transcription factor that labels RGCs. In all cases, cell nuclei are counterstained using DAPI. The *Phr1* mutant retinas appear grossly normal in size, structure, thickness of cellular and plexiform layers, and expression of the appropriate molecular markers for cells and synapses. No quantitative or qualitative differences were observed between genotypes; note that slight variations due to angle of sectioning or retinal curvature are normal and are observed in controls as well. Bar = 50 μm in A–C; 80 μm in E–H.

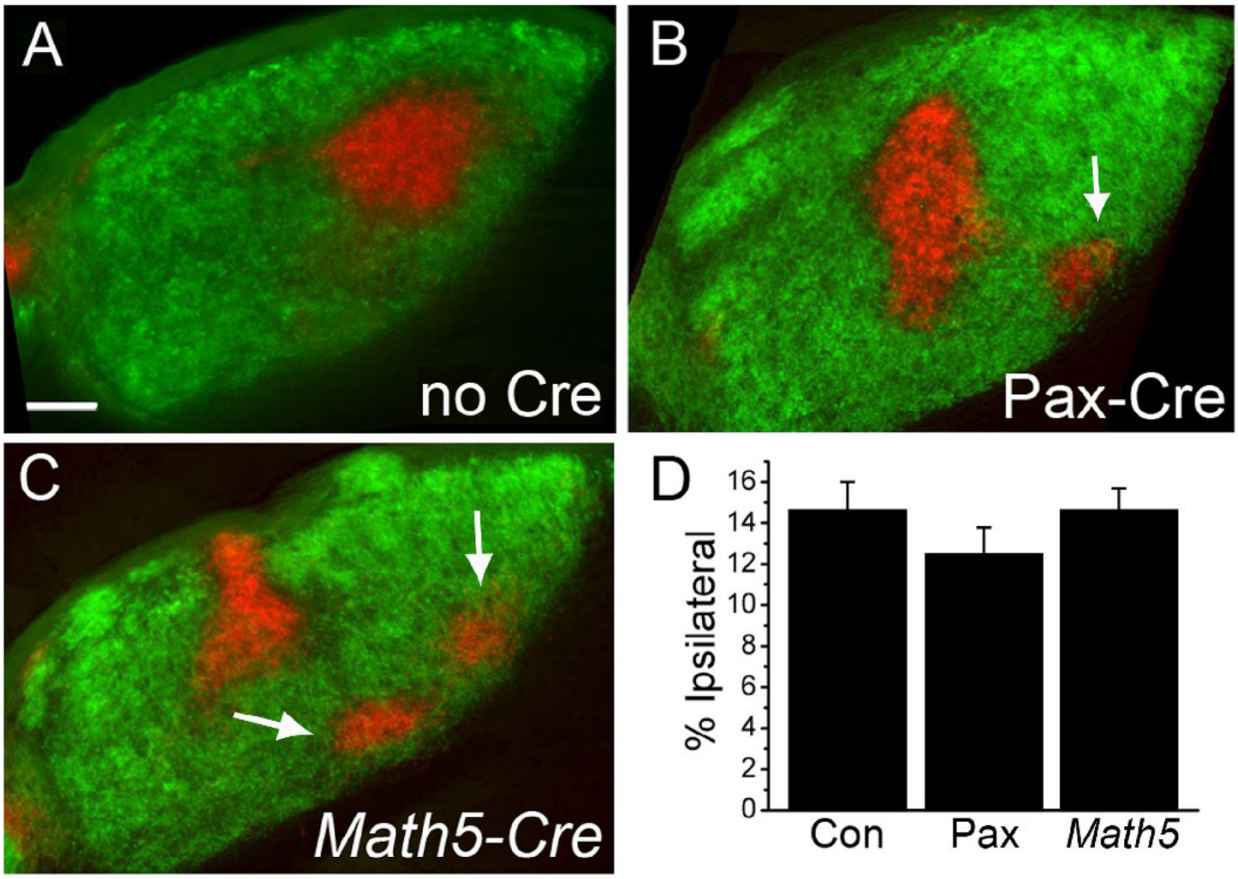

Figure 2.

Phr1 retinal mutants demonstrate defective localization of eye specific patches in the mature dLGN. (**A**) Following injection of labeled CTB into the ipsi- (red) and contralateral (green) eyes, control animals display a stereotyped pattern of innervation of the dLGN from each eye. (**B,C**) This pattern is disrupted in retinal *Phr1* knockouts generated using the retina-specific Pax-Cre or the RGC-ubiquitous *Math5-Cre* lines and the *Phr1* floxed allele. The ipsilateral patch is disrupted into multiple smaller patches (arrows). (**D**) The percentage of the nucleus occupied by ipsilaterally projecting axons is the same in controls (Con) and both *Phr1* retinal mutants (Pax, *Math5*). Scale bar = 100 μm.

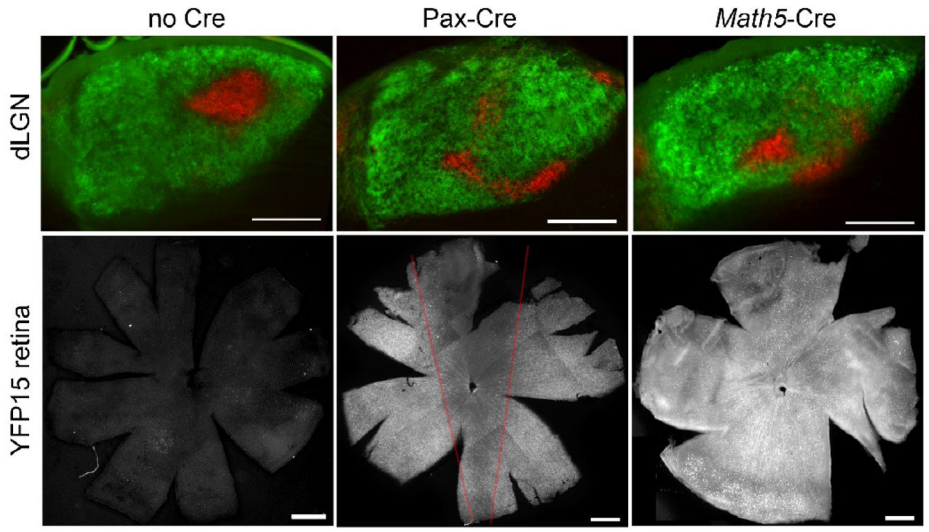

Figure 3.

Phr1 retinal mutants were generated using two different retinal expressing Cre lines. Control animals (no Cre) display a stereotyped pattern of innervation of the dLGN from each eye following injection of labeled CTB into the ipsi- (red) and contralateral (green) eyes. This pattern is disrupted in retinal *Phr1* knockouts generated using the retina-specific Pax-Cre or the RGC-ubiquitous *Math5*-Cre lines and the *Phr1* floxed allele (LGN; arrows). In the absence of Cre the retina demonstrates no fluorescence above background when crossed into the reporter line YFP15 (Buffelli et al., 2003). Pax-Cre expresses in the retina with reduced expression in in a dorsal-ventral wedge (red lines; see also Stacy et al., 2005). *Math5*-Cre expresses throughout the entire retina. Note that in the Pax-Cre line the inferotemporal retina, where the ipsilaterally projecting RGCs reside (see Figure 5), has high expression, likely explaining the similarity of the ipsilateral projection phenotype between the two Cre lines. Scale bars = 200 μm.

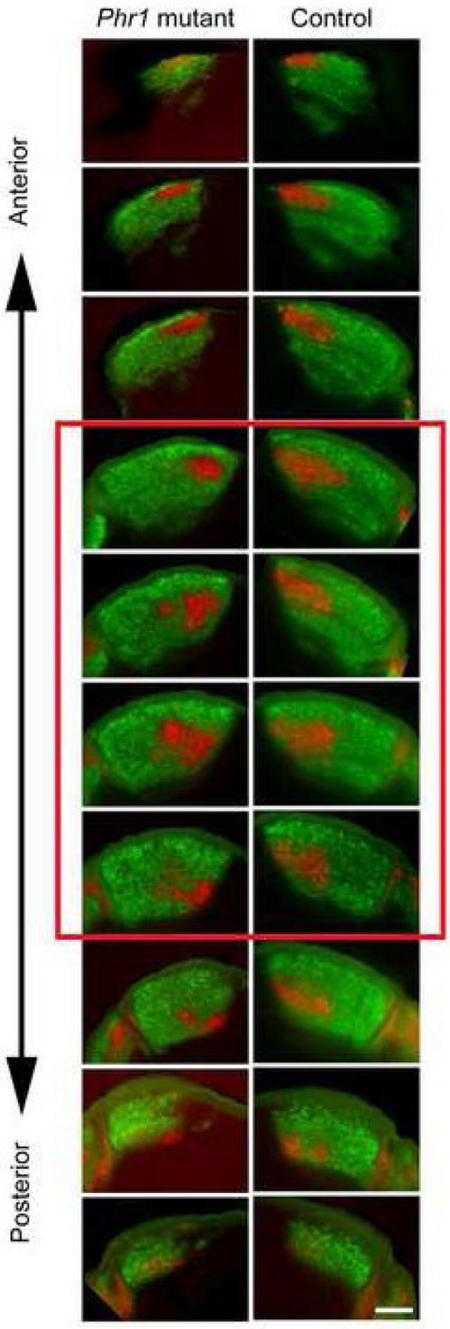

Figure 4.

Quantification of size and overlap of projections. Calculations for both the size of the ipsilateral projection and the R-value distribution for any individual animal were obtained using the average value of 3 to 5 successive sections through the middle of the LGN (red square). The number of images used was determined by discarding the 3 most anterior sections and most posterior sections. Using this approach we found no difference in the area occupied by the ipsilateral patch in *Phr1* retinal mutants vs. controls (see Fig 2). Because the ipsilateral patch is milocalized in the *Phr1* retinal mutant, we performed a second analysis comparing the *volume* of the ipsilateral projection in the mutants and controls by calculating the area occupied by the ipsilateral projection for *all* images through the LGN, divided by the nucleus area in the

same sections. Even with this alternate approach we found no significant difference (14.72% +/− 1.62% no Cre, n=3; 12.58% +/− 1.37% *Math5*-Cre, n=4). Scale bar = 200 μm.

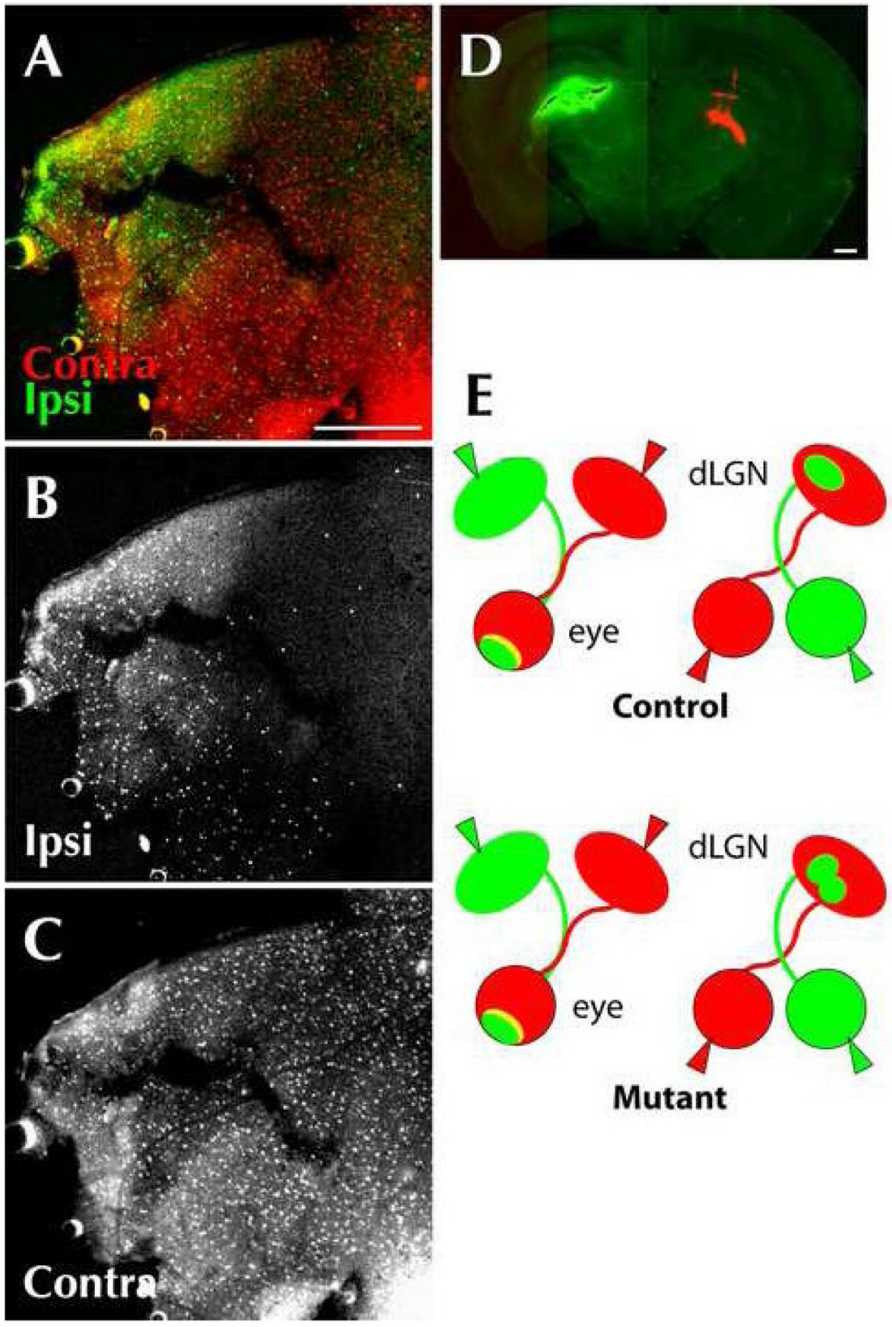

Figure 5.

RGCs from the inferotemporal retina innervate the ipsilateral thalamus in *Phr1* retinal mutants. RGCs from the inferotemporal retina most often innervate the ipsilateral LGN, whereas RGCs from the remainder of the retina usually send axons across the optic chiasm and innervate the contralateral side. (**A, B, C**) Retrograde transport of CTB to the retina of *αPax-Cre Phr1* mutant adult animals after injection of labeled choleratoxin. (**D**) Coronal section of the thalamus from the same animal showing conjugated CTB in the right (green) and left (red) thalamus. Flat mount of the retina of the right eye shows transport of CTB from the ipsilateral (green; A,B) and contralateral (red; A,C) thalamus of *Phr1* retinal mutants. Note that despite a better fill of the CTB injection on the ipsilateral side (green), only the inferotemporal retina was labeled,

unlike the contralateral injection (red) which resulted in labeling across the entire retina. This confirms that axons in the ipsilateral thalamus primarily originate from cell bodies in the inferotemporal retina, as expected. (**E**) Summary of eye and brain injection experiments: When the eyes of *Phr1* retinal mutants are labeled (right) with two different colors, the pattern of label in the dLGN is altered compared to controls. However, when dLGNs are labeled (left), the pattern of label in the retinas is the same for mutants and controls, indicating that the result of the eye labeling experiment is not due to altered axonal crossing of the optic chiasm. Scale bars = 400 μm.

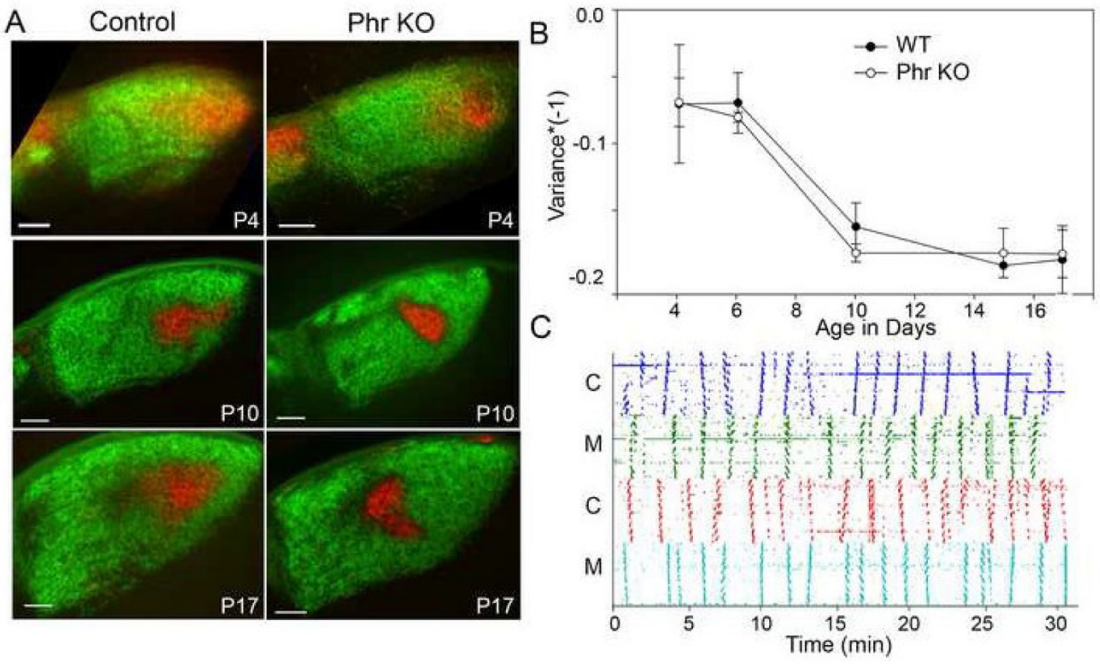

Figure 6.

Segregation and retinal wave activity is normal in *Phr1* retinal KOs. (**A**) CTB labeled ipsi- (red) and contralateral (green) retinal projections in 80 μm coronal dLGN sections from control and Pax6-Cre, *Phr1* mutant mice littermates at three time points showing progression of segregation. (**B**) The time course of segregation was analyzed using the threshold-independent variance of R-value distributions (Torborg and Feller, 2004) and is indistinguishable in mutants and littermate controls. (**C**) *Phr1* retinal mutants generate spontaneous retinal waves. Activity from correlated RGCs using multielectrode array recordings (Demas et al., 2003) over a period of thirty minutes in control (C) and *Phr1* retinal mutant (M) retinas from littermates at P10. Between activity bursts there are quiet stretches with uncorrelated spontaneous activity. Scale bars = 100 μm.

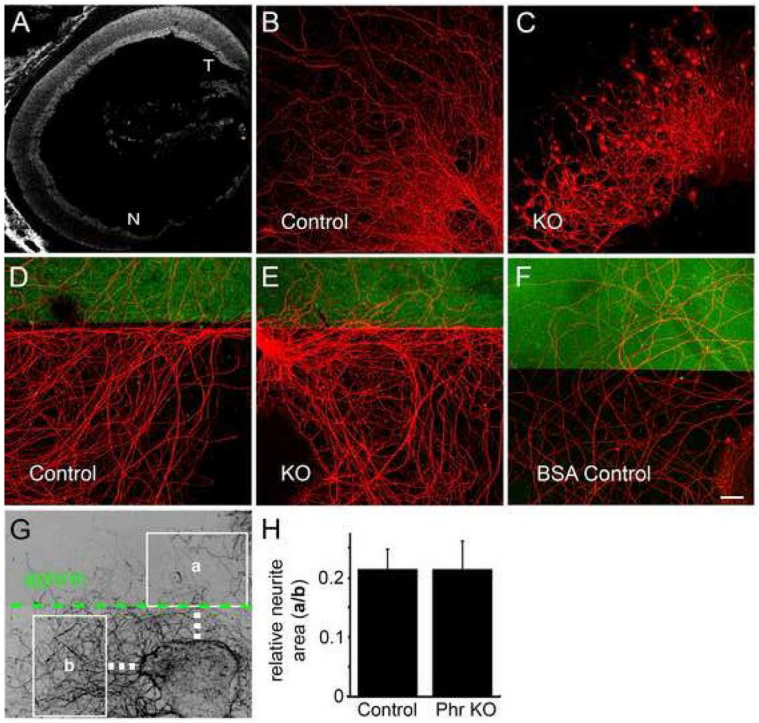

Figure 7.

Mutant axons display morphological defects but respond normally to an ephrin-A border. (**A**) Retinal EphA gradient is preserved in *Phr1* mutants. E18 constitutive *Phr1* knockout retina hybridized with recombinant human Ephrin-A5/Fc as described previously (Feldheim et al, 1998). Like control animals, this shows a nasal-temporal Eph receptor gradient in the *Phr1* mutant retina (T=temporal, N=nasal). (**B,C**) Axons from control and constitutive *Phr1* knockout retinal explants dissected at E16 and cultured for 14 days, stained with anti-neurofilament. (**D,E**) Control and constitutive *Phr1* knockout RGC axons avoid an Ephrin A2 border (marked in green); explants were dissected at E16, cultured 8 days and stained with anti-neurofilament (red). (**F**) No border avoidance was seen with a BSA-only border (green) control. (**G**) Ephrin-A border avoidance was measured as the area of neurites covering a region of ephrin substrate (a) divided by the area of neurites in an equivalent ephrin-free region (b). Quantification is shown in (**H**). Scale bar = 20 μm.